
ELSEVIER

Available at WWW.MATHEMATICSWEB.ORG POWERED BY SCIENCE DIRECT®

Journal of Computational and Applied Mathematics 155 (2003) 405–421

JOURNAL OF COMPUTATIONAL AND APPLIED MATHEMATICS

www.elsevier.com/locate/cam

Algebraic multigrid for complex symmetric matrices and applications☆

Stefan Reitzinger[a,*], Ute Schreiber[b], Ursula van Rienen[b]

[a] *Institute for Computational Mathematics, University of Linz, Linz A-4040, Austria*
[b] *Institute of General Electrical Engineering, University of Rostock, Germany*

Received 22 July 2002; received in revised form 10 October 2002

Abstract

This paper is concerned with the numerical study of an algebraic multigrid preconditioner for complex symmetric system matrices. We use several different Krylov subspace methods as an outer iteration, namely the QMR method proposed by Freund and Nachtigal, the BiCGCR method of Clemens, and the CSYM method of Bunse-Gerstner and Stoever. In addition, we compare the results with the standard Jacobi preconditioner for complex symmetric problems. We test our approach on the numerical simulation of high-voltage insulators.
© 2003 Elsevier Science B.V. All rights reserved.

Keywords: Algebraic multigrid; Electro-quasistatics; Finite integration technique; Complex symmetric matrices; Krylov subspace methods; Preconditioning technique

1. Introduction

In this paper, we consider boundary value problems of second-order elliptic partial differential equations with complex coefficients and appropriate boundary conditions. There are several areas of applications [13]. However, our particular interest consists in the efficient solution of electro-quasistatic problems, a special case of Maxwell's equations, e.g., [16]. The fields are slowly varying with 50 Hz and the displacement current is a significant quantity. As an example, we use

☆ This work has been supported by the Austrian Science Fund—'Fonds zur Förderung der wissenschaftlichen Forschung (FWF)'—under the grant P14953 'Robust Algebraic Multigrid Methods and their Parallelization' and by the German Science Foundation—Deutsche Forschungsgemeinschaft (DFG)—under the projects RI814/10-1 and RI814/10-3 'Numerical Study of Humid Contaminations on Electrically Stressed Polymeric Insulator Surfaces'.
* Corresponding author.
E-mail addresses: reitz@numa.uni-linz.ac.at (S. Reitzinger), ute.schreiber@etechnik.uni-rostock.de (U. Schreiber), ursula.van-rienen@etechnik.uni-rostock.de (U. van Rienen).

0377-0427/03/$ - see front matter © 2003 Elsevier Science B.V. All rights reserved.
doi:10.1016/S0377-0427(02)00877-4

the simulation of electric field strength and force density around water droplets on high-voltage insulators. An insulating system in some high-voltage equipment has to withstand high electric stress for decades. An inherently critical zone of these equipments is the interface between the solid insulator and its surrounding (air plus single water droplets). Hence, the study of the fundamental phenomena in electrically stressed interfaces is of crucial importance to enable the design of high voltage equipments which better satisfy given requirements. The underlying partial differential equation is a potential equation with complex coefficients.

For discretization of the problem we use the finite integration technique (FIT, see [6,29,32]). FIT was developed as a physically based numerical method to solve Maxwell's equations. Using a pair of dual grids the duality between electric and magnetic fields is transferred to the discretization. The consistency of the method answers all physical laws and field properties to hold also in discretization space where the so-called Maxwell's Grid Equations are solved. The discretization yields a complex symmetric linear system, i.e.,

$$\underline{K}_h \underline{u}_h = \underline{f}_h$$

with $\underline{K}_h = K_{\mathrm{h}}^r + \mathrm{i}K_{\mathrm{h}}^i \in \mathbb{C}^{N_h \times N_h}$ the sparse, symmetric system matrix (where $\mathrm{i} = \sqrt{-1}$), $\underline{f}_h \in \mathbb{C}^{N_h}$ the given right-hand side and $\underline{u}_h \in \mathbb{C}^{N_h}$ the coefficient vector of unknowns. Moreover, we assume the real part $K_{\mathrm{h}}^r \in \mathbb{R}^{N_h \times N_h}$ and the imaginary part $K_{\mathrm{h}}^i \in \mathbb{R}^{N_h \times N_h}$ of $\underline{K}_h$ to be symmetric positive definite, i.e., $\underline{K}_h$ is positive stable. The number of unknowns is denoted by N_h and it is related to the discretization parameter h (mesh width) by $N_h = \mathcal{O}(h^{-d})$ in the case of a uniform discretization, where d is the spatial dimension. Hence, N_h becomes very large if h is decreased in order to reduce the discretization error. In addition, the condition number of K_{h}^r and K_{h}^i behaves typically like $\mathcal{O}(h^{-2})$ as h tends to zero. Let us mention that the condition number of K_{h}^i behaves much better than $\mathcal{O}(h^{-2})$ in many practical cases.

The fast and efficient solution of linear systems of equations is a key task in the solution process in many practical applications arising in science and engineering. In the case of nonlinear or optimization problems, linear systems have to be solved repeatedly as part of an outer iteration loop, e.g., a Newton iteration. If the size of such systems (i.e., the number of unknowns) grows, it is important to use algorithms of optimal complexity. Both, memory and time consumption should be proportional to the number of unknowns. Krylov subspace methods together with multigrid-based preconditioners fulfill these requirements. Algebraic multigrid (AMG) methods are of special interest if a geometric multigrid method cannot be applied. There are at least two reasons for using AMG: The discretization provides no hierarchy of meshes or the coarsest grid of a geometric multigrid method is too large to be solved efficiently by a direct or classical iterative solver [1,12,23]. In contrast to geometric multigrid methods where a grid hierarchy is required explicitly, AMG constructs the matrix hierarchy and prolongation operators just by knowing single grid information. In this way, systems with up to several millions of unknowns can be handled even on single processor computers nowadays. It is worth to mention that a complete geometric multigrid proof of this problem class is missing. However, the numerical studies are very meaningful. There are several sequential AMG methods like [2,14,17,19,27,30,31] which differ in their setup phase, i.e., the construction of the matrix hierarchy and of the prolongation operators. They are constructed for real system matrices. The multigrid cycle is then realized in the classical way and performs well if all components are properly chosen. An AMG method for the

complex symmetric case was proposed in [21] for a 2D finite element discretization with nodal elements.

We propose an AMG method which is based on a general approach [10,25] and is therefore applicable to almost every discretization scheme. It can be easily extended to edge element discretization [25,26] or to standard nodal discretizations [25]. Let us mention that the ingredients for an AMG method are the same as for the real case, i.e., coarsening procedure, prolongation/restriction operators, coarse grid operator and smoothing operator. While the prolongation/restriction operators are defined purely real and the coarse grid operator is usually realized by the Galerkin method, the smoothing operator has to be properly adapted to the complex case.

The proposed AMG preconditioner is used in the following together with three Krylov subspace methods: QMR by Freud and Nachtigal [9], BiCGCR by Clemens [5,7], and CSYM by Bunse-Gerstner and Stoever [4].

The paper is organized as follows: In Section 2 we describe the problem and the discretization with FIT. Section 3 is devoted to the algebraic multigrid preconditioner. In Section 4 we present results with the AMG and Jacobi preconditioner for several Krylov subspace methods and finally we draw conclusions in Section 5.

2. Problem formulation and properties

The Maxwell equations [13,16,29,32], which are given by the differential equations:

$$\operatorname{curl} \underline{\vec{H}} = \underline{\vec{J}} + \frac{\partial \underline{\vec{D}}}{\partial t}, \tag{1}$$

$$\operatorname{curl} \underline{\vec{E}} = -\frac{\partial \underline{\vec{B}}}{\partial t}, \tag{2}$$

$$\operatorname{div} \underline{\vec{D}} = q, \tag{3}$$

$$\operatorname{div} \underline{\vec{B}} = 0, \tag{4}$$

are the mathematical model of magnetic and electric fields in a continuum. Therein, $\underline{\vec{H}}$ denotes the magnetic field strength, $\underline{\vec{E}}$ the electric field strength, $\underline{\vec{D}}$ the electric field density, $\underline{\vec{B}}$ the magnetic induction, $\underline{\vec{J}}$ the current density and q the charge carrier density. In addition, appropriate boundary and interface conditions have to be defined. Further the material relations

$$\underline{\vec{J}} = \underline{\vec{J}}_{\mathrm{I}} + \sigma \cdot \underline{\vec{E}} = \underline{\vec{J}}_{\mathrm{I}} + \underline{\vec{J}}_{\mathrm{E}}, \tag{5}$$

$$\underline{\vec{D}} = \varepsilon \cdot \underline{\vec{E}}, \tag{6}$$

$$\underline{\vec{B}} = \mu \cdot \underline{\vec{H}} \tag{7}$$

must hold, with $\underline{\vec{J}}_{\mathrm{E}}$ is called the eddy currents and $\underline{\vec{J}}_{\mathrm{I}}$ describes the impressed current density plus the convection current density. The nonlinear, time-dependent rank-two tensors σ, ε and μ are assumed to be piecewise constant functions with $\sigma \geqslant 0$, $\varepsilon > 0$ and $\mu > 0$ ($\nu = \mu^{-1}$) if it is not stated differently.

2.1. The electro-quasistatic case

Fortunately, in the treatment of slowly varying systems, it is generally not necessary to consider the full set of Maxwell's equations. An electromagnetic field can be considered as slowly varying if the wavelength is large compared to the problem region which means

$$|kR| \ll 1,$$

where R is the characteristic dimension of the system, and $|1/k|$ is the spatial wavelength (a function of the circular frequency ω and the material parameters ϵ, σ, μ). The complex expression for the wave number k reads as

$$k = \omega\sqrt{\mu\varepsilon\left(1 - \mathrm{i}\,\frac{\sigma}{\omega\varepsilon}\right)}.$$

For instance, considering the insulator problem in Section 4.2.1 we find dimensions leading to $R \approx 0.1$ m. Thus, we obtain in that case the estimate

$$|kR| \approx 2 \cdot 10^{-6}, \ldots, 1 \cdot 10^{-7}$$

and consequently the electro-quasistatic problem formulation is legitimate.

In case of $|kR| \ll 1$ it can be assumed that the time-derivative of the magnetic flux is negligible whereas the displacement currents have to be taken into account, i.e.,

$$\partial\underline{\vec{B}}/\partial t = 0, \qquad \partial\underline{\vec{D}}/\partial t \neq 0.$$

Under these assumptions a set of simplified Maxwell's equations for time harmonic electromagnetic fields follows

$$\operatorname{curl}\underline{\vec{E}} = -\partial\vec{B}/\partial t = 0, \tag{8}$$

$$\operatorname{curl}\underline{\vec{H}} = \mathrm{i}\omega\underline{\vec{D}} + \sigma\underline{\vec{E}} + \underline{\vec{J}}_{\mathrm{I}}, \tag{9}$$

$$\operatorname{div}\underline{\vec{D}} = \rho, \tag{10}$$

$$\operatorname{div}\underline{\vec{B}} = 0. \tag{11}$$

For a time harmonic field $\vec{E}(\vec{r},t) = \vec{E}(\vec{r})\cos(\omega t + \Phi)$ we use the representation $\vec{E}(\vec{r},t) = \mathrm{Re}(\underline{\vec{E}}(\vec{r})\mathrm{e}^{\mathrm{i}\omega t})$ with the complex amplitude $\underline{\vec{E}}(\vec{r}) = \vec{E}(\vec{r})\mathrm{e}^{\mathrm{i}\Phi}$. Under these conditions and with Eqs. (8)–(11) we get the complex divergence equation

$$\operatorname{div}((\mathrm{i}\omega\epsilon + \sigma)\underline{\vec{E}}) = -\operatorname{div}(\underline{\vec{J}}_{\mathrm{I}}).$$

According to (8) the electric field $\underline{\vec{E}}$ is curl free and thus may be described as the gradient of a scalar potential. Note that this is a complex potential, i.e.,

$$\underline{\vec{E}} = -\operatorname{grad}\underline{\varphi}.$$

So, the final relation for the electric scalar potential in electro-quasistatics is given by

$$\operatorname{div}((\mathrm{i}\omega\epsilon + \sigma)\operatorname{grad}\underline{\varphi}) = \operatorname{div}(\underline{\vec{J}}_{\mathrm{I}}). \tag{12}$$

2.2. Discretization by the finite integration technique

The finite integration technique (FIT) has been specifically developed for the solution of Maxwell's equations (see [32]). The goal of this development was to achieve a consistent scheme with the ability to solve numerically the complete system of Maxwell's equations in full generality. FIT converts Maxwell's equations in integral form onto a grid pair $(G, \tilde{G})$. This yields a system of linear equations, the so-called Maxwell's Grid Equations. FIT deals with three types of linear operators, the curl-matrices $C, \tilde{C}$, the divergence-matrices $S, \tilde{S}$, and the material matrices $D_\epsilon, D_\mu, D_\sigma$ (see [6,29]). In the electro-quasistatic case, FIT transforms the continuous equation (12) into the discretized one

$$\tilde{S}(\mathrm{i}\omega D_\epsilon + D_\sigma)\tilde{S}^{\mathrm{T}}\underline{\Phi}_{\mathrm{E}} = \tilde{S}\underline{j}_0.$$

The notation

$$A_\sigma := \tilde{S}D_\sigma\tilde{S}^{\mathrm{T}}, \qquad A_\epsilon := \tilde{S}D_\epsilon\tilde{S}^{\mathrm{T}}, \qquad \underline{p}_0 := \tilde{S}\underline{j}_0$$

leads to the resulting complex linear system for our quasi-static field calculations

$$(A_\sigma + \mathrm{i}\omega A_\epsilon)\underline{\Phi}_{\mathrm{E}} = \underline{p}_0. \tag{13}$$

Note that the real part of the complex symmetric matrix $\underline{A} = A_\sigma + \mathrm{i}\omega A_\epsilon$ is just the matrix A_σ for stationary currents and the imaginary part is the matrix A_ϵ of electrostatics, scaled with the frequency ω.

Remark 1. (1) The discretization of such problem could also be done by the finite element method, see, e.g., [21]. The system matrix is essentially the same.

(2) The matrices $A_\sigma, A_\epsilon \in \mathbb{R}^{N_h \times N_h}$ are symmetric positive definite since Dirichlet boundary values are imposed, hence $\underline{A}$ is positive stable.

3. AMG for the complex symmetric case

In order to solve (13) by means of some AMG method or some AMG preconditioned Krylov subspace method, the multigrid constituents have to be defined properly. For further discussion, it suffices to discuss the construction of these components for the two-grid algorithm, for which the indices h and H are related to the fine and coarse grid quantities, respectively. We use the general notation

$$\underline{K}_h\underline{u}_h = \underline{f}_h$$

with

$$\underline{K}_h = K_{\mathrm{h}}^r + \mathrm{i}K_{\mathrm{h}}^i,$$

where

$$K_{\mathrm{h}}^r,\ K_{\mathrm{h}}^i \in \mathbb{R}^{N_h \times N_h}$$

are symmetric positive definite. The case where either K_{h}^r or K_{h}^i is symmetric positive semidefinite is also included.

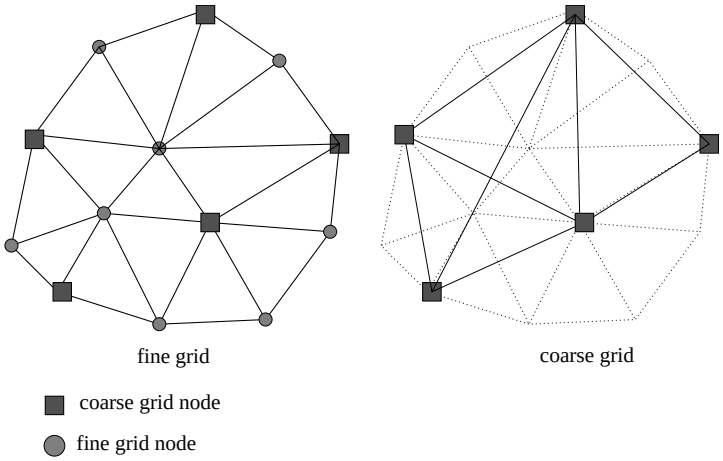

Fig. 1. Detail view of a fine and coarse 'virtual' mesh.

3.1. General concept

Similar to geometric multigrid methods, the efficient interplay of the smoothing process and the coarse grid correction is the crucial point for an efficient AMG method too (see, e.g., [11]). The main difference compared to geometric multigrid methods is the lacking grid hierarchy. In order to come along with that deficiency a coarsening strategy is introduced which decreases the number of unknowns. Most coarsening techniques are based on the matrix graph, see, e.g., [2,3,19,27,30]. Since these approaches are designed for real sparse matrices we cannot directly apply them to the complex system matrix $\underline{K}_h$. Instead we use the general approach proposed in [10,25]. Therefore, we have to specify an auxiliary matrix $B_h \in \mathbb{R}^{N_h \times N_h}$ which represents the underlying mesh.

Meanwhile let us assume that B_h is a sparse M-matrix and that each diagonal entry of B_h can be related to some unknown and therefore to some node or element. There are only local connections to the neighbors. Since this auxiliary matrix is defined locally we are able to define the following index set on a pure algebraic level (with ω_h the set of grid points or elements on level h):

$$N_h^i = \{j \in \omega_h : |(B_h)_{ij}| \neq 0, i \neq j\},$$

$$S_h^i = \{j \in N_h^i : |(B_h)_{ij}| > \text{coarse } (B_h, i, j),\ i \neq j\},$$

$$S_h^{i,T} = \{j \in N_h^i : i \in S_h^j\},$$

which are related to the set of neighbors around a node $i \in \omega_h$, the set of strong connections, and the set of nodes with a strong connection to node i, respectively. Moreover, the function coarse (B_h, i, j) is an appropriate cut-off or coarsening function (see [25]). In an analogous way, the above relations are defined on the coarse grid H provided the matrix B_H is known.

The next step consists in a standard coarsening on B_h. Motivated by some grid (see Fig. 1), a 'virtual' grid can be split into coarse grid nodes ω_C and fine grid nodes ω_F, i.e.,

$$\omega_h = \omega_C \cup \omega_F, \qquad \omega_C \cap \omega_F = \emptyset,$$

such that there are (almost) no direct connections between any two coarse grid nodes. Furthermore, the resulting number of coarse grid nodes should be as large as possible. Then, the coarse grid is simply defined by

$$\omega_H = \omega_C.$$

Remark 2. (i) Note that $B_h \equiv K_h^r$ is an appropriate choice for the auxiliary matrix for our problem class.

(2) The coarse grid selection can be done by several different coarsening strategies (see [2,19,27,30]). On the one hand, a pure matrix graph-based method can be used [2,19], or on the other hand, a coarsening method depending on the matrix entries can be introduced [27,30]. The latter case has the chance to detect anisotropies.

In order to construct a coarse auxiliary matrix we use the well-known Galerkin projection method, and, therefore, we need an appropriate prolongation operator $P_h^B : \mathbb{R}^{N_H} \mapsto \mathbb{R}^{N_h}$, where $N_h = |\omega_h|$ and $N_H = |\omega_H|$ ($N_H < N_h$) denote the number of unknowns on the fine and coarse level, respectively. Once the prolongation operator P_h^B is defined, the auxiliary coarse grid matrix becomes

$$B_H = (P_h^B)^T B_h P_h^B.$$

The efficient interplay of the coarse grid correction and the smoothing procedure is the key ingredient for every multigrid method. This fact is due to the decomposition into the direct sum

$$\mathbb{C}^{N_h} = \mathrm{im}(P_h^K) \oplus \ker((P_h^K)^T),$$

with the full rank prolongation operator P_h^K for the system matrix. This means that the smooth error components (elements in $\mathrm{im}(P_h^K)$) can be well approximated on the coarse grid, while the high frequency components (elements in $\ker((P_h^K)^T)$) must be efficiently reduced by the smoother (see [22,25]). Appropriate smoothers for such kind of problems are the damped complex Jacobi or the complex Gauss–Seidel method.

One possibility to define the prolongation operators P_h^K and P_h^B consists in an equal choice, i.e., $P_h^K \equiv P_h^B \equiv P_h \in \mathbb{R}^{N_h \times N_H}$ which are pure real. For instance, the prolongation operator P_h is defined by the relation

$$(P_h)_{ij} = \begin{cases} 1, & i = j \in \omega_C, \\ \frac{1}{|\omega_C \cap S_h^{i,T}|}, & i \in \omega_F,\ j \in \omega_C, \\ 0 & \text{else.} \end{cases}$$

In the last formula, we assume the coarse grid unknowns to be ordered first. Other prolongation operators are defined, e.g., in [2,19,27,30,14,17,31] that could be used. The coarse system matrix $\underline{K}_H$ is also constructed via Galerkin's method, i.e.,

$$\underline{K}_H = P_h^T \underline{K}_h P_h = P_h^T K_h^r P_h + \mathrm{i} P_h^T K_h^i P_h = K_H^r + \mathrm{i} K_H^i.$$

A recursive application of that process immediately leads to a matrix hierarchy with the corresponding transfer operators. If an appropriate smoothing process is defined, then a complete multigrid V-cycle

can be assembled as is shown in Algorithm 1. The variable CoarseLevel stores the number of levels generated by the coarsening process until the size of the system is smaller than a certain number.

Algorithm 1 V(ν_F, ν_B)-cycle: MG($\underline{u}_\ell, \underline{f}_\ell, \ell$)

if $\ell = COARSELEVEL$ **then**
  Define $\underline{u}_\ell = (\underline{K}_\ell)^{-1}\underline{f}_\ell$ by some direct solver
else
  Smooth ν_F times on $\underline{K}_\ell\underline{u}_\ell = \underline{f}_\ell$
  Calculate the defect $\underline{d}_\ell = \underline{f}_\ell - \underline{K}_\ell\underline{u}_\ell$
  Restrict the defect to the next coarser level $\ell+1$: $\underline{d}_{\ell+1} = P_\ell^{\mathrm{T}}\underline{d}_\ell$
  Set $\underline{u}_{\ell+1} \equiv 0$
  Call MG($\underline{u}_{\ell+1}, \underline{d}_{\ell+1}, \ell+1$)
  Prolongate the correction $\underline{s}_\ell = P_\ell\underline{u}_{\ell+1}$
  Update the solution $\underline{u}_\ell = \underline{u}_\ell + \underline{s}_\ell$
  Smooth ν_B times on $\underline{K}_\ell\underline{u}_\ell = \underline{f}_\ell$
end if

4. Numerical studies

For the calculation of a three-dimensional structure, the number of unknowns N_h of the system matrix $\underline{K}_h$ in (13) is usually of order $\mathcal{O}(h^{-3})$ as the mesh size parameter h tends to zero. In addition, the real and imaginary part of $\underline{K}_h$ has a condition number of order $\mathcal{O}(h^{-2})$. Thus, we require an application of iterative methods in the solution process. We are going to investigate several iterative methods with the AMG and Jacobi preconditioner for the solution of the discretized complex symmetric potential problem. Both preconditioners are implemented in the software package PEBBLES [24]. Other preconditioners showed to be too expensive by negligible advantage (see [7]).

An important class of iterative methods for solving the complex symmetric problems are the following Krylov-subspace methods.

(1) The first method we investigated is the bi-orthogonal conjugate gradient conjugate residual method (BiCGCR), proposed by Clemens, which is a symmetric variant of the BiCG algorithm. An explicit description of this Krylov-subspace method, references and a detailed investigation for complex symmetric systems with similar results can be found in [5,7].
(2) The second investigated method is the quasi-minimal residual method (QMR) of Freund and Nachtigal [9]. The two-term version of this method using the Jacobi-preconditioner with minimal residual smoothing is more stable than the classical three-term version.
(3) Third, an iterative method by Bunse-Gerstner and Stoever [4] which exploits the complex symmetric matrix structure of the system is investigated. This method is called CSYM and is based on unitary equivalence transformations of the system matrix to a tridiagonal form. The algorithm creates a sequence of orthonormal vectors by a three-term recurrence relation, similar to the Lanczos method.

Table 1
CPU times and number of iterations for the unit square $\sigma = 1$

	N_h	Setup (sec)	Solver (sec)	Total time (sec)	No. of iter.
AMG-QMR	10,201	0.84	1.56	2.40	9
	40,401	3.00	7.13	10.1	10
	160,801	11.8	29.2	41.0	10
AMG-BiCGCR	10,201	0.84	1.94	2.78	9
	40,401	3.00	8.82	11.8	10
	160,801	11.8	35.8	47.6	10
AMG-CSYM	10,201	0.84	—	—	>500
	40,401	3.00	—	—	>500
	160,801	11.8	—	—	>500

The convergence criterium is given by

$$\|\underline{f}_h - \underline{K}_h \underline{u}_h^n\|_0 \leqslant \varepsilon \cdot \|\underline{f}_h\|_0$$

for all Krylov-subspace methods. The variable ε denotes the relative accuracy and n is the iteration index of the Krylov method. Moreover, we abbreviate by

$$\rho_h = h_{\max}/h_{\min}$$

the ratio of the maximal to the minimal mesh size.

4.1. A model problem

Our first problem is related to the 2D unit square, i.e., $\Omega = (0,1)^2$ and we assume on $[0,1] \times \{0\}$ homogeneous Dirichlet boundary conditions. On the rest of the boundary, we prescribe homogeneous Neumann boundary conditions. We assume $K_{\mathrm{h}}^r \equiv K_{\mathrm{h}}^i \in \mathbb{R}^{N_h \times N_h}$ and the system matrix is given by

$$\underline{K}_h = K_{\mathrm{h}}^r + \mathrm{i}\sigma K_{\mathrm{h}}^i.$$

The matrices are assembled by the finite element method with bilinear finite element functions. Calculations were done on an SGI Octane, 300 MHz with $\varepsilon = 10^{-8}$ and $\rho_h = 1$.

The results for different values of σ are given in Tables 1–3. In every table, we compare the three Krylov subspace methods preconditioned with the proposed AMG method. The results show a very similar behavior of the QMR and BiCGCR method, whereas the CSYM method hardly converges. However, QMR as well as BiCGCR are robust with respect to the parameter σ. In addition, it is an open question how to construct an efficient preconditioner for CSYM.

Table 2
CPU times and number of iterations for the unit square $\sigma = 10^{+4}$

	N_h	Setup (sec)	Solver (sec)	Total time (sec)	No. of iter.
AMG-QMR	10,201	0.84	1.56	2.40	9
	40,401	3.00	7.14	10.1	10
	160,801	11.8	29.0	40.8	10
AMG-BiCGCR	10,201	0.84	1.93	2.77	9
	40,401	3.00	8.86	11.9	10
	160,801	11.8	36.1	47.9	10
AMG-CSYM	10,201	0.84	—	—	>500
	40,401	3.00	—	—	>500
	160,801	11.8	—	—	>500

Table 3
CPU times and number of iterations for the unit square $\sigma = 10^{-4}$

	N_h	Setup (sec)	Solver (sec)	Total time (sec)	No. of iter.
AMG-QMR	10,201	0.84	1.54	2.38	9
	40,401	3.00	7.08	10.1	10
	160,801	11.8	28.9	40.7	10
AMG-BiCGCR	10,201	0.84	1.93	2.77	9
	40,401	3.00	8.87	11.9	10
	160,801	11.8	36.1	47.9	10
AMG-CSYM	10,201	0.84	—	—	>500
	40,401	3.00	—	—	>500
	160,801	11.8	—	—	>500

4.2. Simulation of electric fields on high-voltage insulators

4.2.1. Description of the example

High-voltage insulators are stressed by the applied electric field as well as by other environmental factors. As a result of this stress, the surface of the insulating material gets aged and the dielectric material looses its hydrophobic and insulating characteristics. The contamination of the object with water droplets accelerates the aging process. Experimental investigations have shown that with increase of applied voltage, droplets vibrate first, they are then extended to the direction of the applied electric field and finally flash over bridging water droplets occurs. To improve the understanding of the aging phenomenon it seems advisable to observe single droplets on an insulating surface. The shape of the droplets supplies more information about the status of the insulating material see

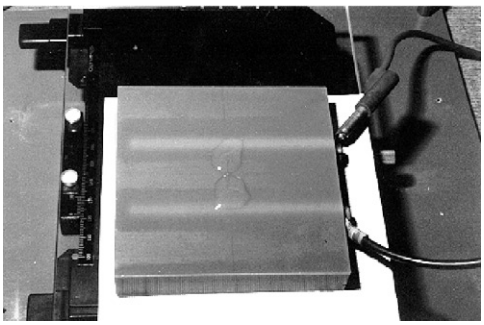

Fig. 2. Two water droplets after 20 min application of high voltage (8 kV). The droplets are deformed during the experiment.

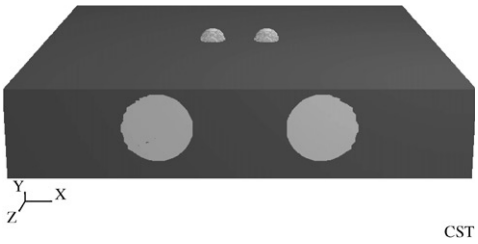

Fig. 3. Model of unaged solid epoxy resin sample with horizontally embedded electrodes and two water droplets on the test object.

[18]. In addition to the experiments [20] the simulation of the electric field strength near the water droplets is necessary. It allows to calculate the electric forces on the droplet surfaces and thus to find a correlation between the shapes and the droplet movement [28]. For experimental investigations of droplet movements it is necessary to eliminate other parameters which influence the distribution of field strength on the insulating surface. This is why simplified test specimen (blocks of epoxy resin) are used for experiments (see [15]) and simulations. Fig. 2 shows the experimental setup and Fig. 3 the test object with two water droplets. In future, practically used test specimen (see Fig. 4) and industrial HV-insulators will be studied too. The considered high-voltage devices are driven with 50 Hz AC voltage, i.e., the electromagnetic field is slowly varying. We model our problem as an electro-quasistatic 3D problem. The epoxy resin has a relative permittivity of $\epsilon_r = 4$ and a conductivity of $\sigma = 10^{-12}$ S/m. The water drops have a relative permittivity of $\epsilon_r = 81$ and a conductivity of $\sigma = 10^{-6}$ S/m. The permittivity of the air surrounding the structure is $\epsilon_r = 1.000576$. A voltage of 15 kV is used (Fig. 5).

For discretization we use FIT on an orthogonal grid. Our insulator problem leads to an almost singular complex symmetric system of linear equations. The matrix is a band matrix with seven bands. The large condition number mainly results from large differences in the material parameters. We are going to investigate the introduced iterative methods and preconditioners for the solution of the discretized potential problem. The electro-quasistatic model is implemented in the software package MAFIA [8] which is based on FIT. Geometric modelling, creation of the complex symmetric

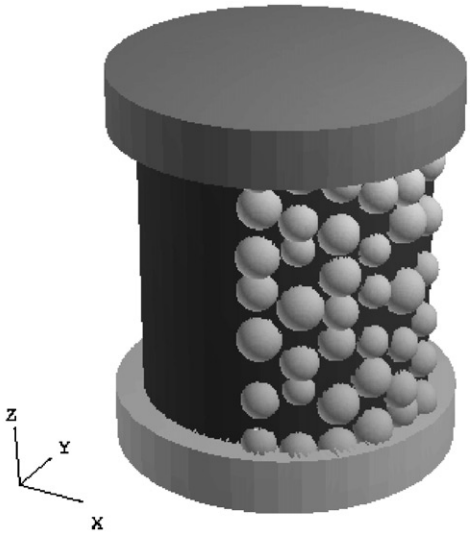

Fig. 4. Industrial test specimen partly covered with single water droplets.

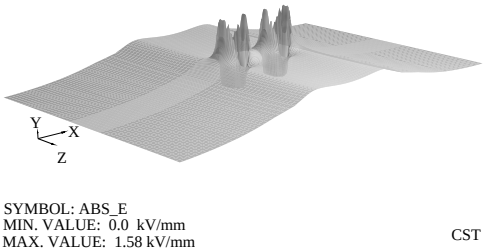

Fig. 5. Magnitude of electric field strength on the epoxy resin sample as shown in Fig. 3.

system of equations and post-processing of the HV examples in this paper are done with this package. The preconditioned iterative solvers are implemented in the PEBBLES software [24] described in Section 3. All calculations were done on a sparc SUN, Ultra-1 with 296 MHz.

4.2.2. Numerical results

Further we tested the introduced algorithms for the two sample objects shown above, the epoxy resin block with two water droplets (see Fig. 3) and the cylindrical test specimen with some water droplets (see Fig. 4). The accuracy ε is set to 10^{-10}.

Example 1. The first sample is a block of epoxy resin with length and width of 100 mm and a height of 20 mm. The test object has horizontally embedded electrodes with a center distance of 35 mm and a radius of 7.5 mm. We put only two droplets on it with a diameter of 6 mm (hemispheres) and a center distance of 10 mm according to the accompanying experiments. The discretization yields a system of 450,241 complex unknowns and a global mesh size ratio $\rho_h = 1$.

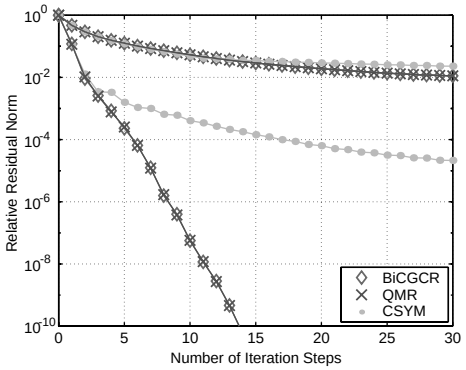

Fig. 6. Results for Example 1: Comparison of iterative algorithms, upper three curves: Jacobi preconditioner, lower three curves: AMG preconditioner.

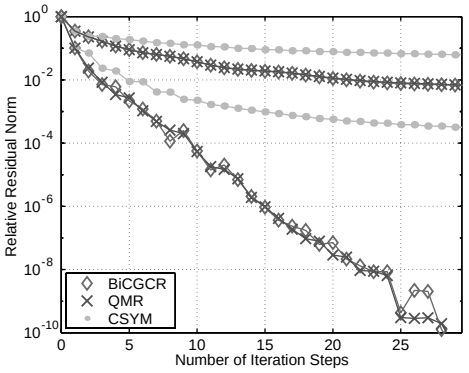

Fig. 7. Results for Example 2: Comparison of iterative algorithms, upper three curves: Jacobi preconditioner, lower three curves: AMG preconditioner.

Example 2. The second model is a cylinder with height of 30 mm and a radius of 15 mm. The electrodes on top and bottom have cylindrical shape too with height of 6 mm and a radius of 18 mm. The droplet radii vary from 1 to 2.5 mm. The discretization yields a system of 145,512 complex unknowns and a global mesh size ratio of $\rho_h = 6$ (Figs. 6, 7, 8 and 9).

Example 3. Example 1 with 12,635 complex unknowns and a global mesh size ratio $\rho_h = 4$.

Example 4. Example 1 with 2541 complex unknowns and a global mesh size ratio $\rho_h = 1$.

The characteristic convergence behavior for the methods can be seen in Figs. 6 and 7. As in the model problem we see in these realistic problems too that the Krylov subspace methods QMR and BiCGCR connected with the AMG-preconditioner PEBBLES perform very similar with respect to the number of iterations. The assumption that the CSYM-algorithm combined with PEBBLES is more applicable than in combination with the Jacobi preconditioner is not verified. Additionally,

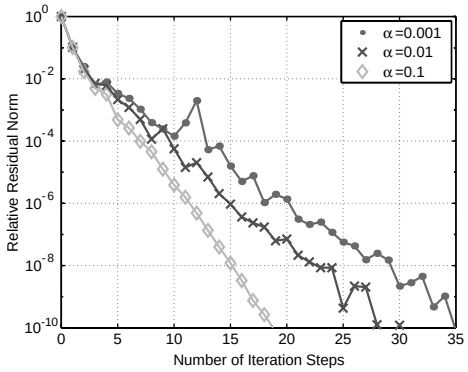

Fig. 8. AMG-QMR for Example 2 with different coarsening factors α.

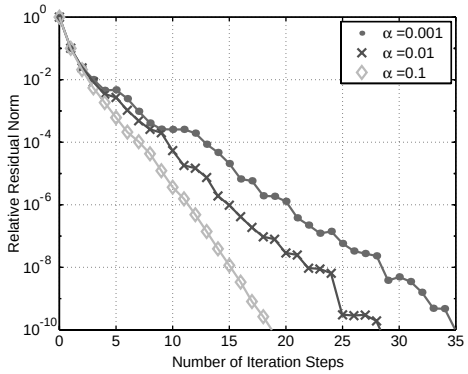

Fig. 9. AMG-BiCGCR for Example 2 with different coarsening factors α.

Table 4
Example 1, $N_h = 450,241$, 6 levels, $\alpha = 0.01$, $\rho_h = 1$

	ε	Setup (sec)	Solver (sec)	Total time (sec)	No. of iter.
AMG-BiCGCR	10^{-10}	187.77	703.44	891.21	15
AMG-QMR	10^{-10}	186.83	493.21	680.04	15
AMG-CSYM	10^{-10}	187.14	>2000	>2000	>65
Jacobi-BiCGCR	10^{-2}	10.45	856.15	866.60	41
Jacobi-QMR	10^{-2}	10.43	810.17	820.60	40
Jacobi-CSYM	10^{-2}	10.61	1390.01	1400.62	90

the comparison of Figs. 6 and 7 leads to the proposition that the number of iteration steps depends more on the condition number of the system (the global mesh size ratio) than on the dimension of the problem. This fact is also reflected in Tables 4 and 5 where CPU times are additionally specified. Overall, the AMG preconditioner accelerates the iteration process in spite of the relatively

Table 5
Example 2, $N_h = 145,512$, 5 levels, $\alpha = 0.01$, $\rho_h = 6$

	ε	Setup (sec)	Solver (sec)	Total time (sec)	No. of iter.
AMG-BiCGCR	10^{-10}	64.43	468.58	533.01	30
AMG-QMR	10^{-10}	64.47	311.47	375.94	30
AMG-CSYM	10^{-10}	64.39	> 2000	> 2000	> 200
Jacobi-BiCGCR	$5 \cdot 10^{-3}$	3.11	848.73	851.84	123
Jacobi-QMR	$5 \cdot 10^{-3}$	3.19	645.12	648.31	104
Jacobi-CSYM	10^{-2}	3.11	1399.72	1402.83	273

Table 6
AMG-QMR, all four examples, $\varepsilon = 10^{-10}$, $\alpha = 0.01$

N_h	ρ_h	Setup (sec)	Solver (sec)	Cycle (sec)	Total time	No. of iter.	Level
2541	1	1.20	1.14	0.114	1.25	10	3
12,635	4	8.51	17.69	1.179	18.87	15	4
145,512	6	64.47	311.47	10.382	321.86	30	5
450,241	1	186.83	493.21	32.881	526.09	15	6

Table 7
AMG-BiCGCR, all four examples, $\varepsilon = 10^{-10}$, $\alpha = 0.01$

N_h	ρ_h	Setup (sec)	Solver (sec)	Cycle (sec)	Total time	No. of iter.	Level
2541	1	1.22	1.67	0.167	1.84	10	3
12,635	4	8.54	16.53	1.102	17.632	15	4
145,512	6	64.43	468.58	15.619	484.20	30	5
450,241	1	187.77	703.44	46.896	750.34	15	6

large setup times compared to classical iterative solvers. Sometimes the Jacobi preconditioner does not reach acceptable accuracies in a reasonable amount of CPU time while mostly PEBBLES solves the problem fast and with high accuracy.

In Tables 6 and 7 the typical properties of PEBBLES are visible. The setup CPU-time, the cycle CPU-time and the used levels principally depend on the problem dimension. The global mesh size ratio ρ_h (and so the condition number) additionally influence the number of needed iterations and thus the solver CPU-time, too.

Remark 3. The coarsening factor α, which is responsible for number of necessary levels and for the dimensions of the reduced problems, intensively influences the solver. For smaller α the total CPU-time grows in spite of lower setup times and the convergence curve gets slightly oscillatory.

5. Conclusions

In this paper, it was shown that the AMG technology allows to construct a good preconditioner for the complex symmetric case. The numerical studies show that our preconditioner is almost optimal with respect to the arithmetic costs. With respect to memory it is optimal and for real life applications it is favorable compared to the classical iterative solvers.

References

[1] O. Axelsson, Iterative Solution Methods, 2nd Edition, Cambridge University Press, Cambridge, 1996.
[2] D. Braess, Towards algebraic multigrid for elliptic problems of second order, Computing 55 (1995) 379–393.
[3] A. Brandt, Generally highly accurate algebraic coarsening, Electromagn. Trans. Numer. Anal. 10 (2000) 1–20.
[4] A. Bunse-Gerstner, R. Stoever, On a conjugate gradient-type method for solving complex symmetric linear systems, Linear Algebra Appl. 287 (1999) 105–123.
[5] M. Clemens, R. Schuhmann, U. van Rienen, T. Weiland, Modern Krylov subspace methods in electromagnetic field computation using the finite integration theorie, Appl. Comput. Electromagn. Soc. J. 11 (1) (1996) 70–84.
[6] M. Clemens, T. Weiland, Discrete electromagnetics: Maxwell's equations tailored to numerical simulations, Internat. Compumag. Soc. Newsletter 8 (2) (2001) 13–20.
[7] M. Clemens, T. Weiland, U. van Rienen, Comparison of Krylov-type methods for complex linear systems applied to high-voltage problems, IEEE Trans. Magn. 34 (5) (1998) 3335–3338.
[8] CST GmbH, Büdinger Str. 2a, D-64289 Darmstadt, MAFIA version 4.020.
[9] R.W. Freund, N.M. Nachtigal, An implementation of the QMR method based on coupled two-term recurrences, SIAM J. Sci. Comput. 15 (1994) 297–312.
[10] G. Haase, U. Langer, S. Reitzinger, J. Schöberl, A general approach to algebraic multigrid, SFB "Numerical and Symbolic Scientific Computing", Technical Report 00-33, Johannes Kepler University Linz, 2000.
[11] W. Hackbusch, Multigrid Methods and Application, Springer, Berlin, Heidelberg, New York, 1985.
[12] W. Hackbusch, Iterative Lösung großer schwachbesetzter Gleichungssysteme, BG Teubner, Stuttgart, 1991.
[13] H.A. Haus, J.R. Melcher, Electromagnetic Fields and Energie, Prentice-Hall, Englewood Cliffs, NJ, 1989.
[14] V.E. Henson, P.S. Vassilevski, Element-free AMGe: general algorithms for computing interpolation weights in AMG, SIAM J. Sci. Comput. 23 (2001) 629–650.
[15] K. Herrbach, Study of behavior of droplets on polymeric surfaces under electrical stress conditions with the aid of a contact angle measuring system, Report, High Voltage Laboratory, University of Technology, Darmstadt, 2000.
[16] N. Ida, J.P.A. Bastos, Electromagnetics and Calculation of Fields, Springer, Berlin, 1997.
[17] J.E. Jones, P.S. Vassilevski, AMGe based on element agglomeration, SIAM J. Sci. Comput. 23 (1) (2001) 109–133.
[18] S. Keim, D. König, Study of the behavior of droplets on polymeric surfaces under the influence of an applied electrical field, IEEE Conference on Electrical Insulation and Dielectric Phenomena (CEIDP), 1999, pp. 707–710.
[19] F. Kickinger, Algebraic multigrid for discrete elliptic second-order problems, Multigrid Methods V, in: W. Hackbusch (Ed.), Proceedings of the Fifth European Multigrid Conference, Springer Lecture Notes in Computational Science and Engineering, Vol. 3, 1998, pp. 157–172.
[20] M. Kneuer, Experimentelle Untersuchungen des Verhaltens von Flüssigkeiten auf Isolierstoffoberflächen unter dem Einflußeines elektrischen Feldes, Master's Thesis, High Voltage Laboratory, University of Technology, Darmstadt, 2000.
[21] D. Lahaye, H. De Gersem, S. Vandewalle, K. Hameyer, Algebraic multigrid for complex symmetric systems, IEEE Trans. Magn. 36 (4) (2000) 1535–1538.
[22] S.F. McCormick, An algebraic Interpretation of multigrid methods, SIAM J. Numer. Anal. 19 (3) (1982) 548–560.
[23] G. Meurant, Computer solution of large linear systems, in: Studies in Mathematics and its Applications, Vol. 28, Elsevier, Amsterdam, 1999.
[24] S. Reitzinger, PEBBLES—User's Guide, Johannes Kepler University Linz, SFB "Numerical and Symbolic Scientific Computing", 1999, www.sfb013.uni-linz.ac.at.

[25] S. Reitzinger, Algebraic multigrid methods for large scale element equations, Schriften der Johannes-Kepler-Universität Linz, Reihe C—Technik und Naturwissenschaften, no. 36, Universitätsverlag Rudolf Trauner, 2001.
[26] S. Reitzinger, J. Schöberl, An algebraic multigrid method for finite element discretizations with edge elements, Numer. Linear Algebra 9 (2002) 223–238.
[27] J.W. Ruge, K. Stüben, Algebraic multigrid (AMG), in: S. McCormick (Ed.), Multigrid Methods, Frontiers in Applied Mathematics, Vol. 5, SIAM, Philadelphia, 1986, pp. 73–130.
[28] U. Schreiber, U. van Rienen, S. Keim, Simulation of electric field strength and force density on contaminated h-v insulators, Vol. 18, Springer Lecture Notes in Computational Science and Engineering, 2001, pp. 79–86.
[29] U. van Rienen, Numerical methods in computational electrodynamics—linear systems in practical applications, Vol. 12, Springer Lecture Notes in Computational Science and Engineering, 2001.
[30] P. Vanek, J. Mandel, M. Brezina, Algebraic multigrid by smoothed aggregation for second and fourth order elliptic problems, Computing 56 (1996) 179–196.
[31] C. Wagner, On the algebraic construction of multilevel transfer operators, Computing 65 (2000) 73–95.
[32] T. Weiland, A discretization method for the solution of Maxwell's equation for six-component fields, Electron. Commun. AEÜ 31 (3) (1977) 116–120.